Replacement of lateral boundary condition in the operational meso scale model at JMA

Tabito Hara[1], Masami Narita, Ryoji Nagasawa,
Daisuke Miura, and Yutaka Furuichi

Numerical Prediction Division, Japan Meteorological Agency,
1-3-4, Otemachi, Chiyoda-ku, Tokyo 100-8122, Japan

1 Introduction

MSM, the meso scale model at the Japan Meteorological Agency (JMA) with nonhydrostatic model (JMA-NHM), has been operated to issue information for disaster prevention (Saito et al. 2006, 2007). Its horizontal grid spacing is 5 km and it covers the region around Japan, 3600 km from east to west, 2880 km from north to south. Forecasts for 15 hours had been provided every 3-hours until May 2007, forecast period was extended to 33 hours 4 times among 8 times a day with considerable model improvements(Hara et al. 2007). This extension made it possible to deliver information to users up to 24 hours ahead.

Since MSM is a regional model, lateral boundary conditions are necessary to incorporate information outside of the domain. In MSM, the forecasts with RSM (Regional Spectral Model) had been used as the boundary condition since the beginning of its operation in Mar. 2001. On Nov. 21, 2007, RSM was replaced as the model providing the boundary condition by high resolution Global Spectrum Model (20-km GSM) at the same time with the start of the operation of GSM at JMA as the short-term weather forecasting model instead of RSM. GSM delivers its forecasts every 6 hours, while RSM did only twice a day. More frequent update of the boundary condition brings the advantage that MSM can use more accurate boundary condition because of its shorter forecast period and the latest observations assimilated through the analysis system.

In this report, we will present the performance of MSM with 20-km GSM forecasts given as the boundary condition, comparing it with the characteristics of 20-km GSM forecasts. It is confirmed that the performance of the inner model is strongly affected by the characteristics of the boundary condition.

Hereafter, MSM with the boundary condition provided by GSM and RSM are referred to as G-MSM and R-MSM, respectively.

2 New MSM system with 20-km GSM as the boundary conditions

Since Nov. 21, 2007, the forecasts predicted by 20-km GSM have been adopted instead of RSM as boundary conditions for MSM. The boundary conditions are updated every 6 hours corresponding to the update frequency of GSM. The other specifications of MSM are not changed from the previous upgrade in May 2007.

Note that the boundary conditions are also used in Meso-4DVAR analysis system. Although the model is influenced by 20-km GSM only in the boundary regions, the effects brought by 20-km GSM spread over the domain through the analysis cycle.

[1]E-mail: tabito.hara@met.kishou.go.jp

3 Statistical Verifications

To investigate the performance of G-MSM, experiments are conducted for one month for both in summer (Aug. 2004) and in winter (Dec. 2005 – Jan. 2006).

3.1 Vertical profiles

Fig.1 displays the vertical profiles of error statistics against the sonde observations over the MSM region. In the summer, the vertical profiles of root mean square error (RMSE) of geopotential height (Fig.1(a)), temperature, and wind speed (not shown) are improved more in G-MSM than R-MSM, which is attributed to the better performance of 20-km GSM than RSM from the view point of synoptic field. However, it also gives negative impact on MSM such as larger negative bias in vertical profiles of relative humidity (RH) (Fig.1(b)), which seems to be brought by 20-km GSM characteristics which has a considerable dry bias in the middle layer. In the winter, the geopotential height at upper layer around 250-300 hPa has an outstanding negative bias (Fig.1(c)), and the temperature has corresponding positive bias (Fig.1(d)), which are also under the influence of GSM characteristics.

3.2 Precipitation

There are no much differences in the threat score for predicting precipitation between G-MSM and R-MSM (Fig.2(a)). Special attention should be drawn to the increase of frequency to predict precipitation, especially heavy ones which can be recognized from the bias score (Fig.2(b)). It is considered to be brought by the excessive effect of the convective parameterization (Kain-Fritsch scheme) under the drier middle layer and moister lower layer, to which 20-km GSM has similar characteristics. One example of the cases in which precipitation is overestimated by G-MSM is displayed later.

3.3 Quality degradation with the forecast time advancing

As already mentioned, it is more advantageous for G-MSM that more frequently updated forecasts can be used as the boundary condition. Fig.3 shows the time series of threat score for precipitation predicted by G-MSM for each initial time. For several hours from each initial time, the best prediction can be obtained by adopting the latest one. However, in comparison with threat score between G-MSM of 15UTC initial time and G-MSM of 21UTC one, the quality of 21UTC is more rapidly degraded than 15UTC and the accuracy is almost the same in the latter part of forecast in spite of the shorter forecast time of 21UTC than one of 15UTC.

Presumably, the reason may be explained by the hypothesis that GSM of 06UTC and 18UTC initial

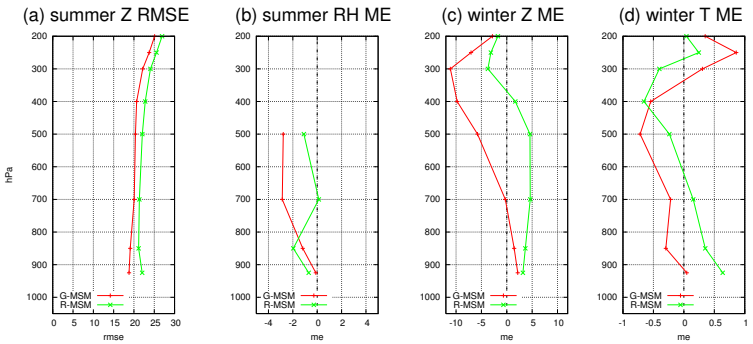

Fig. 1: Vertical Profiles of ME and RMSE. (a) RMSE of geopotential height (Z) [m] in the summer, (b) ME of RH [%] in the summer, (c) ME of Z [m] in the winter, and (d) ME of temperature [°C] in the winter. Green: R-MSM, Red: G-MSM.

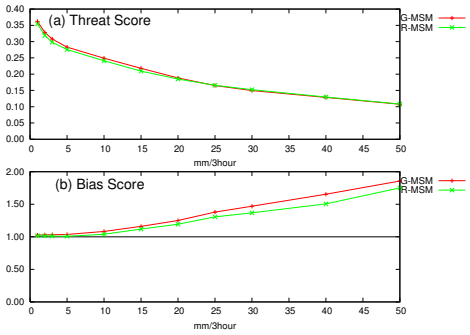

Fig. 2: Scores of precipitation prediction of each threshold. (a) threat score, (b) bias score. The transverse axis indicates threshold of precipitation [mm/3hour].

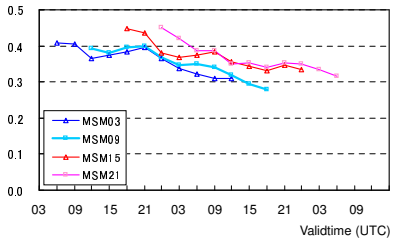

Fig. 3: Time series of threat score of precipitation with threshold of 1mm/3h for each initial time.

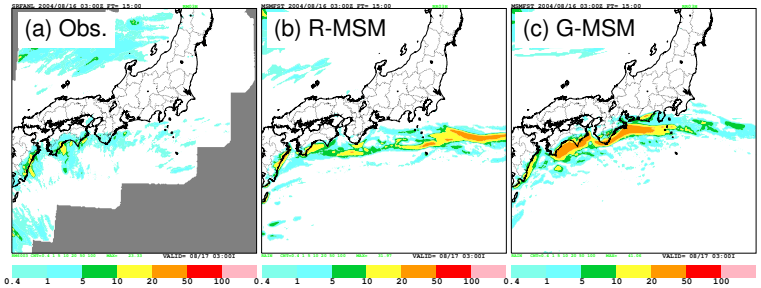

Fig. 4: 3-hour accumulated precipitation predicted with R-MSM and G-MSM, and its corresponding observation. Initial time is Aug. 16, 2004. Forecast time is 15 hours.

time is not as good as GSM of 00UTC and 12UTC due to the constraint of the operational system, in which the first guesses of the data assimilation of 00UTC and 12 UTC are generated by the analysis with more observations than 06UTC and 18UTC.

4 Problematic example predicted with G-MSM

Fig.4 shows the predictions with G-MSM and R-MSM, and the corresponding observation for the case on Aug. 16, 2004. In this case, weak precipitation was observed along the southern coast of Japan in association with the front. While R-MSM predicted similarly to the observation, G-MSM predicted too much precipitation intensity, which was mostly brought by the KF scheme, not grid-scale cloud microphysics. The lower layer in the south of precipitation area in G-MSM was much moister than R-MSM, and 20-km GSM used as the boundary condition of G-MSM had also the similar field to G-MSM, which suggests that G-MSM is considerably affected by moister field of 20km-GSM. It led to the overestimated precipitation by the KF scheme because the moister the lower layer, the more active the KF scheme works.

Although G-MSM do not always predict such excessive precipitation, frequency of it tends to be greater than R-MSM as the bias score of statistical verification (Fig.2(b)) indicates.

5 Conclusion

The boundary condition of MSM was switched to forecasts by 20-km GSM from that by RSM in Nov. 2007. Because of the better performance of 20-km GSM, some improvements are obtained. However, undesirable characteristics of 20-km GSM also affects MSM prediction, such as moist bias at lower layer, dry bias at middle layer, and positive temperature bias at upper layer, as well as the precipitation forecasts. To resolve these problems, 20-km GSM is highly expected to be improved. On the other hand, physical schemes in MSM should be also reviewed to adapt the different characteristics from the former boundary conditions.

References

Hara, T., K. Aranami, R. Nagasawa, M. Narita, T. Segawa, D. Miura, Y. Honda, H. Nakayama, and K. Takenouchi, 2007: Upgrade of the operational JMA non-hydrostatic mesoscale model. *CAS/JSC WGNE Res. Activ. Atmos. Oceanic Modell.*, **37**, 0511–0512.

Saito, K., J. Ishida, K. Aranami, T. Hara, T. Segawa, M. Narita, and Y. Honda, 2007: Nonhydrostatic Atmospheric Models and Operational Development at JMA. *J. Meteor. Soc. Japan*, **85B**, 271–304.

Saito, K., T. Fujita, Y. Yamada, J. Ishida, Y. Kumagai, K. Aranami, S. Ohmori, R. Nagasawa, S. Kumagai, C. Muroi, T. Kato, H. Eito, and Y. Yamazaki, 2006: The Operational JMA Nonhydrostatic Mesoscale Model. *Mon. Wea. Rev.*, **134**, 1266–1298.